

Correction of cavity absorptance measure method for cryogenic radiometer

ISSN 1751-8822

Received on 23rd November 2015

Revised on 17th March 2016

Accepted on 2nd April 2016

doi: 10.1049/iet-smt.2015.0267

www.ietdl.org

 Xiaolong Yi^{1,2}, Wei Fang¹, Yang Luo¹, Zhiwei Xia¹, Yupeng Wang¹ ✉

¹Changchun Institute of Optics, Fine Mechanics and Physics, Chinese Academy of Sciences, Changchun 130033, People's Republic of China

²University of Chinese Academy of Sciences, Beijing 100049, People's Republic of China

✉ E-mail: wangyp@ciomp.ac.cn

Abstract: As the reference detector of absolute radiance calibration primary radiometer (ARCPR) for space remote sensing, total solar irradiance (TSI) cavity is investigated to ensure the measurement accuracy. TSI cavity adopts a sloping bottom cavity. The geometrical parameters and paint material of sloping bottom cavity are both optimised to improve the invariance of absorptance in the environment of ground and space. The optimisation of substitution method is proposed to measure the average absorptance by two-dimensional scan. The uniformity is evaluated by absorptance map. Experimental results illustrate that sloping bottom cavity has a super-high absorptance of 0.999928 (wavelength is 632 nm), and the relative measure uncertainty is approximated to 6 ppm. Meanwhile, compared with the absorptance map of conical cavity, the sloping bottom design improves the uniformity of absorptance. Therefore, the sloping bottom cavity can be adopted as the reference detector of ARCPR. Furthermore, the optimised substitution method is suitable for the investigation of the blackbody cavity with super-high absorptance.

1 Introduction

Radiance calibration method on space platforms has the problem of less precision [1, 2]. Based on the development trend of ground-based radiance calibration [3, 4], the absolute radiance calibration primary radiometer (ARCPR) for space remote sensing is developed for establishing radiance calibration standard on orbit. ARCPR is an electrical-substitution radiometer working at 20 K temperature environment. The sun is the optical source. ARCPR contains total solar irradiance (TSI) cavity and high sensitivity (HS) cavity.

As the reference detector of ARCPR, the TSI cavity is a blackbody absorber, which is used for TSI calibration. Based on the improvement of thermal noise and the application of superconducting technology [5], the relative standard uncertainty of TSI calibration is 200 ppm. Hence, the on-orbit irradiance calibration standard is established by TSI cavity. HS cavity is used to calibrate the solar spectrum irradiance. HS cavity, as well as other remote sensors, can be calibrated by the TSI cavity. Then, the spectrum responses of remote sensors can be calibrated by HS cavity.

The absorptance is a main performance of the blackbody absorber, which is widely used as standard radiation sources or detectors in radiometry and radiation thermometry [6, 7]. The investigation and optimisation of absorptance mainly rely on computational simulation [8, 9]. The super-high absorptance needs to be verified by experimental method.

To guarantee the low measurement uncertainty of ARCPR, the absorptance of TSI cavity should have a super-high absorptance more than 0.9999 and the measurement uncertainty should be <10 ppm. Besides, the uniformity of absorptance is another important performance of TSI cavity [10]. Most of absorptance measure methods use laser as optical source because of its stability [11]. However, the sun is the optical source of the TSI cavity in practical measurement. Due to the different beam diameters, TSI and laser illuminate different areas on the bottom surface. Thus, the absorptance measure method needs some optimisation.

In this paper, the investigation of TSI cavity is introduced. A cylindrical cavity with an inclined bottom surface (sloping bottom cavity) is manufactured to be used as TSI cavity. The absorptance of sloping bottom cavity is extremely stable in the space or on the

ground. An optimisation substitution method is proposed. In order to verify the super-high absorptance of the sloping bottom cavity, measure equipment is set up based on the optimisation substitution method. The uniformity of absorptance is evaluated by two-dimensional scan. Then the absorptance of sloping bottom cavity is measured. Meanwhile, measurement uncertainty is analysed. The feasibility of using sloping bottom cavity as TSI cavity is investigated.

2 Sloping bottom cavity design

Sloping bottom cavity consisted of cylindrical prototype, sloping bottom and view-limiting aperture as shown in Fig. 1. Cavity absorptance mainly depended on the parameters, including the conical angle (α), the inclination angle (β), the length of cavity (H) and the black paint absorptivity (ϵ). In practical application, the decline of ϵ is the primary influence factor of absorptance. In order to ensure the absorptance stability in the space and on the ground, sloping bottom cavity is optimised as follows.

2.1 Geometrical parameter optimisation

The sloping bottom cavity is made of oxygen-free copper. In 20 K cryogenic environment, the specific heat capacity of oxygen-free copper is significantly reduced. Thus, the sloping bottom cavity with large volume can also have little thermal time constant. The application of cryogenic technique ensures that the absorptance can be improved by optimising geometrical parameters. Dr. Qianqian Fang's work provides a method for optimising the geometrical parameters [8]. When α and β are both approximated to 30°, the absorptance of sloping bottom cavity is maximum. The improvement of absorptance mainly depended on the increase of reflection times. Therefore, despite ϵ is dropping from 0.9 to 0.7, when H is 40 mm, the absorptance is superior to 0.9999.

2.2 Paint material optimisation

Compared with specular reflection black paint, diffuse black paint has a lower absorptivity: ϵ is 0.75 at 632 nm wavelength.

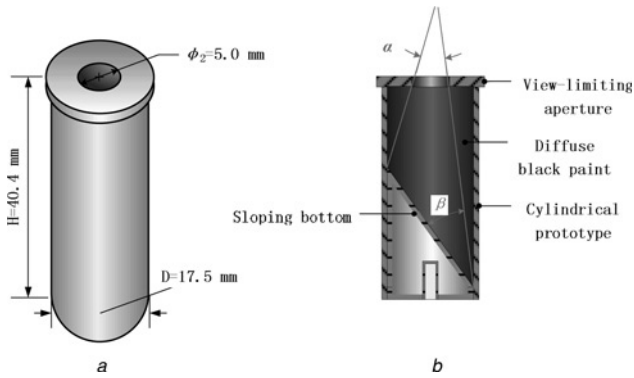


Fig. 1 Sloping bottom cavity design

a Geometrical parameters
b Section drawing

However, the recession of diffuse black paint is almost negligible in the long-term measurement process on orbit [12]. This stable performance is necessary in order to ensure the absolute accuracy of TSI cavity. Therefore, the diffuse black paint is adopted instead of the specular reflection black paint, which is widely used in the conical cavity of TSI monitor on Feng Yun-3 satellites [13–17].

2.3 Performance verification requirements

According to the above optimisations, the stability of super-high absorptance is guaranteed, and sloping bottom cavity is manufactured. The computer simulation of absorptance is realised by Monte Carlo principle and Trace-Pro software [8]. The absorptance of sloping bottom cavity is 0.99995 by computer simulation. The super-high absorptance needs to be verified by experiment. The TSI cavity requires that the absorptance measurement accuracy should be <10 ppm.

Most of absorptance measure method adopts laser as the optical source because of its stability. However, in practical measurement, the sun is the optical source of TSI cavity. TSI and laser illuminate different areas on the bottom surface. Measure method needs some optimisation in order to obtain the practical absorptance.

3 Investigation and optimisation of substitution method

When optical power (P_O) enters the cavity, one part (P_A) is absorbed, the other part (P_R) is reflected. The ratio between P_A and P_O is entitled as absorptance (α). The ratio between P_R and P_O is named as reflectance (ρ). Absorptance is usually measured by substitution method or interchange method [18]. The principle of substitution method is expounded according to integrating sphere theory. Then the substitution method is optimised by the analysis.

3.1 Substitution method principle

Optical source is vertically entering the integrating sphere and then reflected by a sample. Meanwhile silicon photodiode outputs a response voltage (U_X) as shown in Fig. 2. In the first place, sloping bottom cavity (ρ_C) is placed in the sample region, resulting in a response voltage (U_C). Second, sloping bottom cavity is substituted by standard white board (ρ_S), leading to a response voltage (U_S). Finally, standard white board is taken off from sample region. Then optical source passes through the integrating sphere. The response voltage of background is U_B .

According to the integrating sphere theory, the irradiance (E) of inner surface can be calculated by

$$E = \frac{\phi}{\pi A} \times M, \quad (1)$$

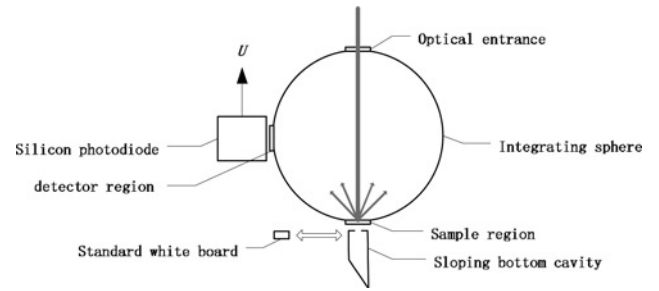


Fig. 2 Principle of substitution method

where ϕ is the incident radiation flux, A is the inner surface area of integrating sphere and M is the integrating sphere factor, which is depicted by

$$M = \frac{\rho_0}{1 - \rho_w(1 - \sum_{n=1}^N f_n) - \sum_{n=1}^N \rho_n f_n}, \quad (2)$$

where ρ_0 is the reflectance of the sample, ρ_w is the reflectance of inner surface of integrating sphere, ρ_n is the reflectance of openings, f_n is the area ratio between openings and integrating sphere inner surface. N is number of openings. The openings of integrating sphere include optical entrance, sample and detector regions. As the total area of openings is far less than integrating sphere inner surface, (2) is simplified as

$$M \simeq \frac{\rho_0}{1 - \rho_w(1 - \sum_{n=1}^N f_n)}, \quad (3)$$

When sloping bottom cavity is installed on sample region, M_C is expressed as

$$M_C = \frac{\rho_C}{1 - \rho_w(1 - \sum_{n=1}^N f_n)}, \quad (4)$$

When standard white board is installed on sample region, M_S is expressed as

$$M_S = \frac{\rho_S}{1 - \rho_w(1 - \sum_{n=1}^N f_n)}, \quad (5)$$

The relationship between E and U is proportional. According to (1), (4) and (5), the proportional relationship is expressed as

$$\frac{U_C - U_B}{U_S - U_B} = \frac{E_C}{E_S} = \frac{M_C}{M_S} = \frac{\rho_C}{\rho_S}, \quad (6)$$

Thus, the absorptance (α_C) of sloping bottom cavity is depicted as

$$\alpha_C = 1 - \rho_C = 1 - \frac{U_C - U_B}{U_S - U_B} \times \rho_S, \quad (7)$$

3.2 Optimisations of substitution method

3.2.1 Response voltage correction: The stability of optical source is a primary influence factor of measurement precision. Laser is used as the optical source in order to improve the stability of optical source. The fluctuation of optical source will reduce the measurement accuracy. Thus, the optical source is monitored in measurement process. Then U is corrected by a reference voltage (u). The corrected value (η) is expressed as

$$\eta = U/u, \quad (8)$$

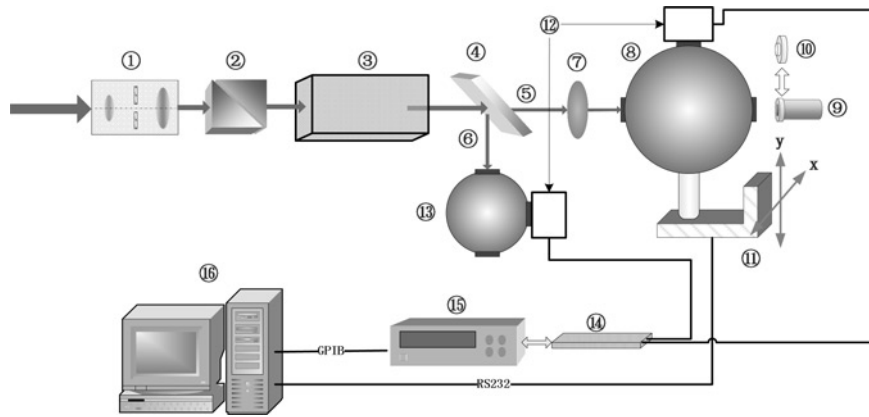


Fig. 3 Measurement equipment: ① spatial filter; ② polariser; ③ power stabiliser; ④ beam splitter; ⑤ single optical path; ⑥ reference optical path; ⑦ converging mirror; ⑧ integrating sphere-I; ⑨ sloping bottom cavity; ⑩ standard white board; ⑪ digital two-dimensional platform; ⑫ detectors; ⑬ integrating sphere-II; ⑭ scanning board; ⑮ digital multi-meter; ⑯ computer and software

According to (7) and (8), α_C can also be calculated by

$$\alpha_C = 1 - \rho_C = 1 - \frac{\eta_C - \eta_B}{\eta_S - \eta_B} \times \rho_S, \quad (9)$$

where η_C is the correction value of sloping bottom cavity, η_S is the correction value of reference white board and η_B is the correction value of background.

3.2.2 Average absorptance: The sun is used as the optical source for sloping bottom cavity. The practical absorptance should be represented by the average absorptance (κ), which is obtained by two-dimensional scan. Then κ is calculated by

$$\kappa = \frac{1}{T} \sum_{x=a}^A \sum_{y=b}^B \alpha_{Cxy} = \frac{1}{T} \sum_{x=a}^A \sum_{y=b}^B \left(1 - \frac{\eta_{cxy} - \eta_{bxy}}{\eta_{sxy} - \eta_{bxy}} \times \rho_S \right), \quad (10)$$

where T is the number of effective sampling points, the position of laser beam at sloping bottom surface is represented by a two-dimensional coordinate (x, y). α_{Cxy} is the absorptance at one position.

4 Measurement experiment

4.1 Equipment setup

Laser ($\lambda = 632 \text{ nm}$) is used as the optical source as shown in Fig. 3. The stability of laser power is improved from 0.1 to 0.02% by spatial filter, polariser and power stabiliser. Then laser power is divided into a single optical path and a reference optical path by beam splitter. Through converging mirror, the single optical path goes into integrating sphere-I for measuring absorptance. Converging mirror is adopted to adjust the spot diameter of single optical path. The spot diameter is adjusted to 1 mm at the incidence plane of sloping bottom cavity.

The reference optical path goes into integrating sphere-II in order to monitor laser power stability. U and u are both obtained through detectors (Hamamatsu S1406-6), and sampled by digital multi-meter (Keithley 2700) and scanning board (Keithley 7700). Integrating sphere-I is installed on a digital two-dimensional platform.

4.2 Automatic control software

Data acquisition and scanning process realise computer automatic control. Automatic control software is developed by LabVIEW. Sampling frequency is set to 1 Hz. The communication between computer and digital multi-meter is based on general-purpose interface bus. Digital multi-meter is used to measure and upload

data under computer control. The communication between computer and digital two-dimensional platform is based on serial bus (RS-232). The software controls two-dimensional platform to move integrating sphere-I with sloping bottom cavity.

5 Measurement result and accuracy analysis

5.1 Absorptance measurement result

The experiment process is performed in the dark room. The response voltages of sloping bottom cavity, reference white board and background are, respectively, scanned through the above equipment. Laser scan covers an area of $6.0 \times 6.0 \text{ mm}^2$ with a resolution of 0.2 mm, producing a sample map. Then according to the two vertical tangent lines of view-limiting aperture, the sample map is reduced to an area of $5.0 \times 5.0 \text{ mm}^2$. The sample maps of response voltages and correction values are shown in Fig. 4.

The absorptance map of sloping bottom cavity is obtained by (9). The absorptance of sloping bottom cavity is superior to 0.9999 as shown in Fig. 5a. The experimental results are determined at one wavelength ($\lambda = 632 \text{ nm}$). According to (10), the average absorptance (κ) is 0.999928 ($\lambda = 632 \text{ nm}$). Thus, the absorptance of sloping bottom cavity is super high and uniform.

The absorptance of a conical cavity is also measured with this equipment. The laser power is vertically reflected at the conical cavity tip. Most of the laser power is directly reflected to the outside of cavity. Meanwhile, due to the limitation of black paint spraying process, the tip cannot be painted as good as the rest of other cavity surface. Thus, the absorptance of conical cavity is lower at the centre of the absorptance map as shown in Fig. 5b. The sloping bottom design solves this problem. Compared with conical cavity, the absorptance of sloping bottom cavity is higher and more uniform. Therefore, the uniformity of absorptance is verified through two-dimensional scanning.

5.2 Measurement accuracy analysis

5.2.1 Relative uncertainty: According to (8) and (9), α_C can be calculated by

$$\alpha_C = 1 - \rho_C = 1 - \frac{U_C/u_C - U_B/u_B}{U_S/u_S - U_B/u_B} \times \rho_S, \quad (11)$$

Then the uncertainty of absorptance ($\sigma(\alpha_C)$) is expressed as (see equation at the bottom of the next page)

where the composition factors are depicted by

$$\frac{\partial \rho_C}{\partial U_C} = \frac{1}{U_S/u_S - U_B/u_B} \cdot \frac{\rho_S}{u_C}, \quad (13)$$

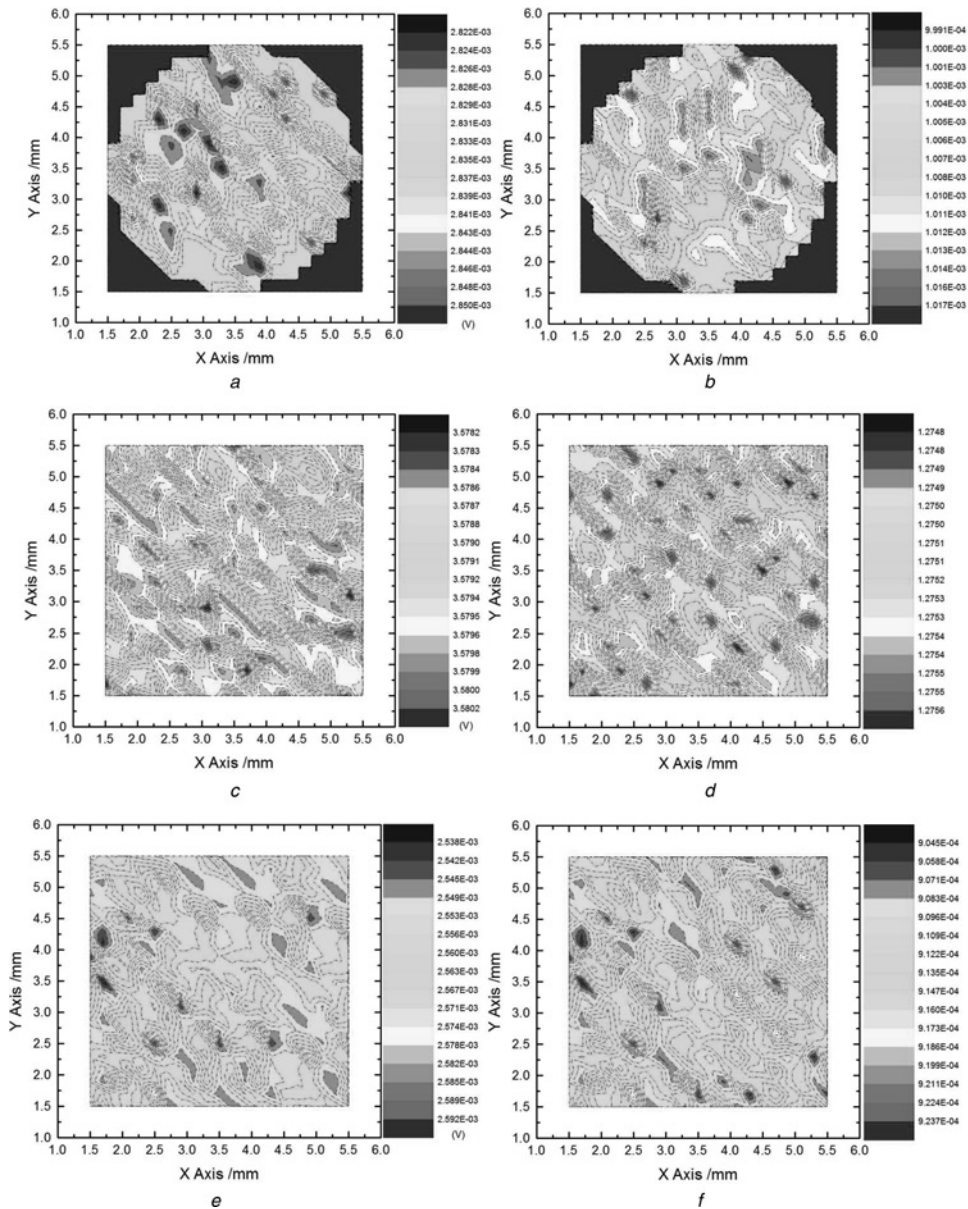


Fig. 4 Measurement result maps

- a* Response voltage of sloping bottom cavity, U_C/V
b Correction value of sloping bottom cavity, η_C
c Response voltage of reference white board, U_S/V
d Correction value of reference white board, η_S
e Response voltage of background, U_B/V
f Correction value of background, η_B

$$\frac{\partial \rho_C}{\partial U_S} = -\frac{U_C/u_C - U_B/u_B}{(U_S/u_S - U_B/u_B)^2} \cdot \frac{\rho_S}{u_S}, \quad (14)$$

$$\frac{\partial \rho_C}{\partial U_B} = \frac{U_C/u_C - U_S/u_S}{(U_S/u_S - U_B/u_B)^2} \cdot \frac{\rho_S}{u_B}, \quad (15)$$

$$\frac{\partial \rho_C}{\partial \rho_S} = \frac{U_C/u_C - U_B/u_B}{U_S/u_S - U_B/u_B}, \quad (16)$$

$$\frac{\partial \rho_C}{\partial u_C} = \frac{-1}{U_S/u_S - U_B/u_B} \cdot \frac{U_C \rho_S}{u_C^2}, \quad (17)$$

$$\frac{\partial \rho_C}{\partial u_S} = \frac{U_C/u_C - U_B/u_B}{(U_S/u_S - U_B/u_B)^2} \cdot \frac{U_S \rho_S}{u_S^2}, \quad (18)$$

$$\frac{\partial \rho_C}{\partial u_B} = \frac{U_S/u_S - U_C/u_C}{(U_S/u_S - U_B/u_B)^2} \cdot \frac{U_B \rho_S}{u_B^2}, \quad (19)$$

Then $\sigma(\alpha_C)$ can be calculated by (12)–(19). The composition factors are achieved as shown in Table 1.

5.2.2 Uncertainty components: Equation (12) illustrates that $\sigma(\alpha_C)$ depended on the uncertainty of response voltages and the reference white board reflectance.

$$\sigma(\alpha_C) = \sqrt{\left(\frac{\partial \rho_C}{\partial U_C}\right)^2 \sigma^2(U_C) + \left(\frac{\partial \rho_C}{\partial U_S}\right)^2 \sigma^2(U_S) + \left(\frac{\partial \rho_C}{\partial U_B}\right)^2 u^2(U_B) + \left(\frac{\partial \rho_C}{\partial \rho_S}\right)^2 \sigma^2(\rho_S) + \left(\frac{\partial \rho_C}{\partial u_C}\right)^2 \sigma^2(u_C) + \left(\frac{\partial \rho_C}{\partial u_S}\right)^2 \sigma^2(u_S) + \left(\frac{\partial \rho_C}{\partial u_B}\right)^2 \sigma^2(u_B)}, \quad (12)$$

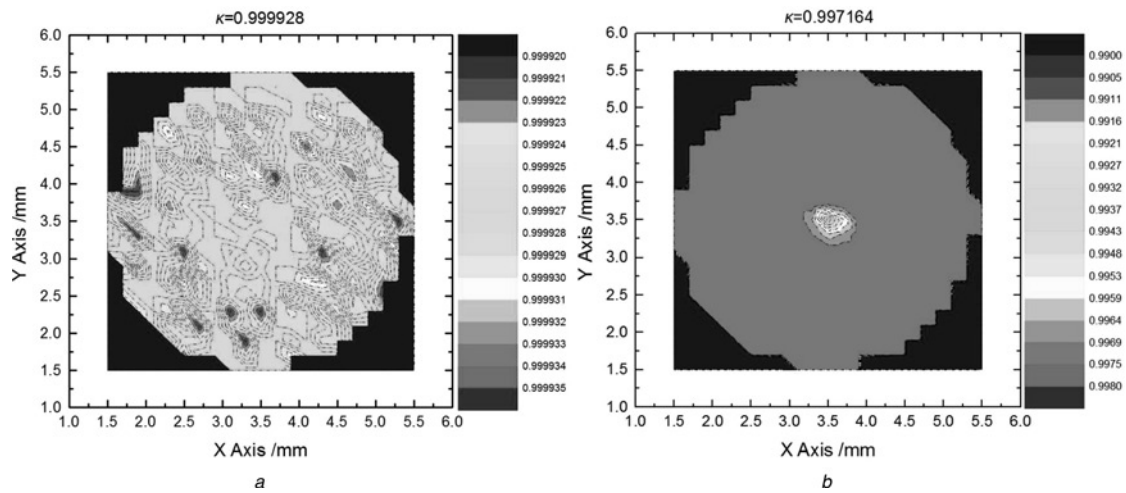


Fig. 5 Absorbance comparison: sloping bottom cavity has a more uniform absorbance. The absorbance of conical cavity is lower in the central core
a Sloping bottom cavity
b Conical cavity

Table 1 Composition factors of absorbance measurement

Parameter	Value	Equation	Calculated value	Parameter	Calculated value
U_C	0.002960	13	0.2658	U_D/U_C	0.001093785
u_C	2.7062	17	-2.935×10^{-5}	U_S/U_S	1.321448365
U_S	3.5765	14	-0.2658	U_B/U_B	0.000947983
u_S	2.7065	18	1.104×10^{-4}		
U_B	0.002566	15	-2.908×10^{-4}		
u_B	2.7068	19	3.878×10^{-5}		
ρ_S	0.95	16	2.519×10^{-4}		

Table 2 Uncertainty components of absorbance measurement

Parameter	Value	σ_{11}	σ_{12}	σ_1	σ_2	Composition factor	Calculated value
U_C	0.002960	6.3×10^{-6}	1×10^{-8}	6.3×10^{-6}		0.2658	2.8×10^{-12}
u_C	2.7062	2.2×10^{-4}	1.8×10^{-4}	2.9×10^{-4}		-2.935×10^{-5}	6.3×10^{-15}
U_S	3.5765	3.9×10^{-4}	2.7×10^{-4}	4.7×10^{-4}		-0.2658	1.9×10^{-16}
u_S	2.7065	3.4×10^{-4}	1.8×10^{-4}	3.9×10^{-4}		1.104×10^{-4}	2.2×10^{-16}
U_B	0.002566	7.6×10^{-6}	1×10^{-8}	7.6×10^{-6}		-2.908×10^{-4}	4.1×10^{-12}
u_B	2.7068	2.2×10^{-4}	1.8×10^{-4}	2.9×10^{-4}		3.878×10^{-5}	5.1×10^{-15}
ρ_S	0.95				0.05	2.519×10^{-4}	3.1×10^{-11}
						combined uncertainty	6.11×10^{-6}

The uncertainty of response voltages (σ_1) is calculated by

$$\sigma_1 = \sqrt{\sigma_{11}^2 + \sigma_{12}^2}, \quad (20)$$

where σ_{11} is the standard deviation of response voltages and σ_{12} is the accuracy of the digital multi-meter. First, σ_{11} is calculated by

$$\sigma_{11} = \sqrt{\frac{1}{n-1} \sum_{i=1}^n (X_i - \eta)^2}, \quad (21)$$

where n is the measurement times, X_i is the response voltages and η is the average value of X_i . Then, σ_{12} is depicted by

$$\sigma_{12} = \eta \times (\eta \times \delta_1 + L \times \delta_2) \times 10^{-6}, \quad (22)$$

where L is the measurement range of digital multi-meter, δ_1 and δ_2 are calibration coefficients. When $L = 0.1$ V, then $\delta_1 = 15$, $\delta_2 = 30$. When $L = 10$ V, then $\delta_1 = 10$, $\delta_2 = 4$.

The reference white board reflectance is calibrated by Changchun Institute of Optics, Fine Mechanics and Physics, and the uncertainty of ρ_S (σ_2) is 0.05.

The uncertainty components are listed in Table 2, and $\sigma(\alpha_C)$ is 6×10^{-6} . Therefore, the relative uncertainty of absorbance is approximated to 6 ppm. Experimental result illustrates that sloping bottom cavity has a super-high absorbance of 0.999928 ± 0.000006 ($\lambda = 632$ nm). The optimisation method satisfies the requirement of absorbance measurement. Meanwhile, the uniformity of absorbance is verified through two-dimensional scanning. Therefore, sloping bottom cavity can be used as the TSI cavity, which is the reference detector of ARCPR.

6 Conclusion

ARCPR is developed for establishing radiance calibration standard on orbit. As the reference detector of ARCPR, the TSI cavity is a blackbody cavity. The absorbance is a main performance of TSI cavity. In order to ensure the high measurement accuracy of ARCPR, TSI cavity should have a super-high absorbance more than 0.9999 and the relative uncertainty is under 10 ppm. Besides, the uniformity of absorbance is another important performance of TSI cavity.

A sloping bottom cavity is manufactured to be used as the TSI cavity. The geometrical parameters and paint material are both

optimised to improve the stability of absorptance in the space and on the ground. The improvement of absorptance mainly depended on the increase of reflection times.

Optimised substitution method is proposed to obtain the average absorptance, which is obtained by two-dimensional scan. Experimental results illustrate that sloping bottom cavity has a super-high absorptance of 0.999928 ($\lambda = 632 \text{ nm}$), and the relative measurement accuracy is approximated to 6 ppm. Meanwhile, compared with the absorptance map of conical cavity, the sloping bottom design improves the uniformity of absorptance. Therefore, TSI cavity can adopt sloping bottom cavity to be used as the reference detector for ARCPR. Furthermore, the optimised substitution method is suitable for the investigation of the blackbody cavity with super-high absorptance.

7 Acknowledgments

The authors thank numerous staffs in Changchun Institute of Optics, Fine Mechanics and Physics, Chinese Academy of Sciences, including Xin Ye, Dongjun Yang, Kai Wang and many others. The authors are grateful to Bingxi Yu, former project leader of SIAR, for his great contributions and guidance. The authors also thank the referee for generous help and good comments. This work was supported by the National Natural Science Foundation of China (NSFC) (no. 41227003 and no. 41474161).

8 References

- 1 Dinguirard, M., Slater, P.N.: 'Calibration of space-multispectral imaging sensors: a review', *Remote Sens. Environ.*, 1999, **68**, pp. 194–205
- 2 Chander, G., Markham, B.L., Helder, D.L.: 'Summary of current radiometric calibration coefficients for Landsat MSS, TM, ETM+, and EO-1 ALI sensors', *Remote Sens. Environ.*, 2009, **113**, pp. 893–903
- 3 Willson, R.C.: 'Active cavity radiometer type IV', *Appl. Opt.*, 1979, **18**, pp. 179–188
- 4 Martin, J.E., Fox, N.P.: 'Cryogenic solar absolute radiometer (CSAR)', *Metrologia*, 1993, **30**, pp. 305–308
- 5 Pearson, D.A., Zhang, A.M.: 'Thermal-electrical modeling of absolute cryogenic radiometers', *Cryogenics*, 1999, **39**, pp. 299–309
- 6 Prokhorov, A.V., Hanssen, L.M.: 'Effective emissivity of a cylindrical cavity with an inclined bottom: I. Isothermal cavity', *Metrologia*, 2004, **41**, pp. 421–431
- 7 Wang, H., Xia, X.: 'Broadband absorptance enhancement of silicon nanowire arrays with germanium as the substrate', *Opt. Eng.*, 2013, **52**, (8), p. 087104
- 8 Fang, Q., Fang, W., Wang, Y., *et al.*: 'New shape of blackbody cavity: conical generatrix with an inclined bottom', *Opt. Eng.*, 2012, **51**, (8), p. 086401
- 9 Gentile, T.R., Houston, J.M., Hardis, J.E., *et al.*: 'National Institute of Standards and Technology high-accuracy cryogenic radiometer', *Appl. Opt.*, 1996, **3**, (7), pp. 1056–1068
- 10 Balasa, I., Jensen, L.O., Ristau, D., *et al.*: 'Laser calorimetric absorptance testing of samples with varying geometry', *Opt. Eng.*, 2014, **53**, (12), p. 122503
- 11 Palm, W.J., Marciniak, M.A., Perram, G.P.: 'Wavelength and temperature dependence of continuous-wave laser absorptance in Kapton thin films', *Opt. Eng.*, 2012, **51**, (12), p. 121802
- 12 Beck, I.: 'Determination of the relative absorbance of cavities for a solar radiometer'. Bachelor-thesis, University of Zurich, 2014
- 13 Fang, W., Wang, H., Li, H., *et al.*: 'Total solar irradiance monitor for Chinese FY-3A and FY-3B satellites – instrument design', *Solar Phys.*, 2014, **289**, pp. 4711–4726
- 14 Wang, H., Li, H., Qi, J., *et al.*: 'Total solar irradiance monitor for the FY-3B satellite-space experiments and primary data corrections', *Solar Phys.*, 2015, **290**, pp. 645–655
- 15 Wang, H., Li, H., Fang, W.: 'Timing parameter optimization for comparison experiments of TSIM', *Appl. Opt.*, 2014, **53**, (9), pp. 1719–1726
- 16 Gong, C., Fang, W.: 'Software design and implementation for solar irradiance monitor on FY-3 A satellite', *Opt. Precis. Eng.*, 2010, **18**, pp. 1476–1482
- 17 Wang, Y., Fang, W., Gong, C., *et al.*: 'Dual cavity inter-compensating absolute radiometer', *Opt. Precis. Eng.*, 2007, **15**, (11), pp. 1662–1667
- 18 Shan, B.: 'Research on the measurement techniques of detector spectral response based on cryogenic radiometer'. PhD thesis, National Institute of Metrology, P. R. China, 2012